
Article:
Benites, Ana Beatriz, Alarcon, Rafael T., Gaglieri, Caroline et al. (2 more authors) (2020) Effect of metal oxide fillers in urethane dimethacrylate polymer with glycerol obtained by photopolymerization synthesis. Journal of Polymer Research. ISSN 1572-8935

https://doi.org/10.1007/s10965-020-02292-1

Effect of metal oxide fillers in urethane dimethacrylate polymer with glycerol obtained by photopolymerization synthesis

Ana Beatriz Benites[1], Rafael T. Alarcon[1], Caroline Gaglieri[1], Katie J. Lamb[2], Gilbert Bannach[1*]

[1]UNESP - São Paulo State University, School of Science, Department of Chemistry, Bauru, São Paulo 17033-260, Brazil

[2]The University of York, Green Chemistry Centre of Excellence, Department of Chemistry, Heslington, York, YO10 5DD, UK

*Corresponding author. E-mail: gilbert.bannach@unesp.br

ORCID:

0000-0002-6249-8698 – Ana Beatriz Benites

0000-0003-2798-9587 – Rafael T. Alarcon

0000-0001-9612-6887 – Caroline Gaglieri

0000-0002-5244-5015 – Katie J. Lamb

0000-0002-8790-5069 – Gilbert Bannach

Acknowledgments The authors thank CAPES (grants 024/2012 and 011/2009 Pro-equipment), FAPESP Grants 2017/08820-8, 2018/03460-6 and 2019/11493-4 São Paulo Research Foundation (FAPESP), and CNPq (grant 301857/2018-0) for financial support. The authors also thank Arthur Rossi de Oliveira for initiating the experiments.

Declarations

Funding: CAPES (grants 024/2012 and 011/2009 Pro-equipment), São Paulo Research Foundation - FAPESP (Grants 2017/08820-8, 2019/11493-4 and 2018/03460-6), and CNPq (grant 301857/2018-0).

Conflicts of interest/ Competing interests: Not applicable.

Availability of data and material: Not applicable.

Code availability: Not applicable.

Abstract

Urethane dimethacrylate (UDMA) is a monomer widely used in photopolymerization reactions to produce biomaterials, due to its advantageous properties such as mechanical resistance and relatively low viscosity. However, this monomer is expensive. Reducing the quantity of UDMA monomer required to obtain the final polymer, without losing its main properties, is essential not just in terms of costs but also green chemistry principles. It has been demonstrated that glycerol inclusion into the polymeric matrix during polymerization is one way to achieve this goal. Thus, this work proposes the insertion of glycerol and metal oxide fillers (Al_2O_3, TiO_2, Nb_2O_5, La_2O_3 and ZrO_2) in the photopolymerization of urethane dimethacrylate, with the aim to study how these effects the degree of conversion, as well as the thermal properties of the final polymer. The thermal properties were evaluated using simultaneous thermogravimetry-differential thermal analysis (TG-DTA) and differential scanning calorimetry (DSC). The degree of conversion/rate of polymerization was calculated using mid-infrared spectroscopy (MIR). The polymers filled with Al_2O_3, TiO_2, Nb_2O_5 and La_2O_3 exhibited good conversion values of 87.42, 78.47, 77.64 and 75.51%, respectively. For all polymers synthesized, no significant changes were observed in their thermal stability. Lastly, it is suggested that the incorporation of the oxides in the monomeric mixture correlate to the degree of conversion, with scanning electronic microscopy (SEM) analysis suggesting oxide dispersion interferes with the morphology of the polymer.

Keywords Photopolymerization; Degree of conversion; Metal oxides fillers; Urethane dimethacrylate; Glycerol.

Introduction

The urethane dimethacrylate (UDMA) monomer is often used in polymeric matrices and composites for biomaterial production, especially in dental restoration resins [1-4]. Urethane dimethacrylate derived polymers present high mechanical resistance, relatively low viscosity, low water absorption and are highly crosslinkable [2,5-7]. In addition, the UDMA monomer can be readily photopolymerized using ultra-violet or visible light by the two-component (Type II) method, in which a photoinitiator molecule is excited at a specific wavelength. Consequently, the excited molecule reaches a different electronic (triplet) state and interacts with the co-initiator, resulting in the cleavage of a C-H bond and thus radical formation. This then starts the radical polymerization process [8-10].

Photopolymerization has several benefits in comparison to the traditional thermal polymerization route. It has a lower environmental impact, producing no pollutant emissions during the process, and is a faster and cheaper synthetic route. This process can be performed at room temperature in a few minutes and requires one of the less energy intensive and broadly accessible radiation sources; visible light [11,12]. All of these positive aspects of photopolymerization are in accordance with the green chemistry principles [13,14].

One of the main issues associated with polymerization is the large amount of monomer required, especially when using expensive monomers such as UDMA. This problem can be tackled by aggregating a polyalcohol into the monomeric mixture in an appropriate proportion, as this can minimize the amount of monomer required to produce the final polymer. This has the added benefit of reducing raw material use and costs without losing the desirable properties of the final polymeric material [15,16]. Glycerol (1,2,3-propanetriol) is a non-toxic polyalcohol in the form of a viscous and odorless liquid, obtained from natural or petrochemical sources [17]. It is also a by-product derived from biodiesel production, which is inexpensive and widely produced in Brazil. According to the Brazilian government, it was estimated in 2018 that biodiesel production generated approximately half a million tons of glycerin, which after undergoing a refinement process forms glycerol [18]. The insertion of glycerol into polymers structure is one way to increase the use of an industrial by-product, whilst also decreasing the quantity of expensive monomers required to produce the final polymer.

Over the last few years, specific studies into analyzing the effects of adding fillers into polymeric structures for biomaterials, such as silica and alkaline glasses, have been performed. These studies noted the importance of particle size, shape and distribution, as well as matrix composition to improve mechanical properties, dental resin applicability and monomeric conversion velocity [19-21]. However, the majority of these studies focused on evaluating the shrinkage, mechanical properties and wear resistance of the polymer. Very few studies report the degree of monomer conversion into a metal oxide-filled polymer and its influence on the thermal properties of the polymer [21-23].

In a previous study, a UDMA-based polymer was successfully synthesized with glycerol added in molar proportions of 1:1, 1:3 and 1:5 UDMA:Glycerol, and the polymer with the maximum ratio of glycerol (1:5) showed a monomer conversion of 67.52% [15]. Therefore, this work aims to study whether or not the conversion degree of the photocured glycerol based UDMA polymer (1:5), reported in our previous work, is enhanced by the addition of different metal oxide fillers into the polymeric structure, especially in terms of its thermal properties. The metal-based oxides Al_2O_3, TiO_2, Nb_2O_5, La_2O_3 and ZrO_2 were selected for

this study due to their white coloration, which means they do not absorb visible light. Consequently, they would not compete with the photosensitizer for light absorption, allowing the photosentizer to reach an excited state and should not interfere in the photopolymerization process.

Experimental

General

All chemicals and metal oxide fillers, including camphorquinone (CQ, 97%), ethyl-*p*-dimethylaminobenzoate (99%), glycerol (99.7%), urethane dimethacrylate (UDMA, ≥ 97%), Al_2O_3 (≥ 99.5%, ⌀ ≤ 10 μm), TiO_2 (≥ 99%, ⌀ ≤ 47 μm), Nb_2O_5 (99.9%, ⌀ ≤ 47 μm), La_2O_3 (99.9%, ⌀ ≤ 200 μm) and ZrO_2 (99%, ⌀ ≤ 5 μm) were provided by Sigma-Aldrich and used without further purification or pre-treatment. The particles size values were obtained from the data sheets provided for each oxide by Sigma-Aldrich. Acetone was provided by Merck (analytical grade).

Preparation of photoinitiator solution

CQ was used as the photoinitiator and solubilized in acetone at a concentration of 0.01 mol (1.6622 g) per 10 mL of acetone. The solution was kept in an amber flask to prevent photodegradation. Subsequently, 0.01 mol (1.9324 g) of the co-initiator ethyl-*p*-dimethylaminobenzoate was added to the solution.

Preparation of the monomeric mixtures

In five different polypropylene container, 0.01 mol (4.7056 g) of UDMA was added to 0.05 mol of glycerol (0.9209 g). Thereafter, a different metal oxide filler (Al_2O_3, TiO_2, Nb_2O_5, La_2O_3 and ZrO_2) was added to each flask (5.0 wt% of the total monomeric mixture). Then, 2 mL of the photoinitiator solution were added to each monomeric mixture. Fig. 1 demonstrates the compounds used to make the monomeric mixtures.

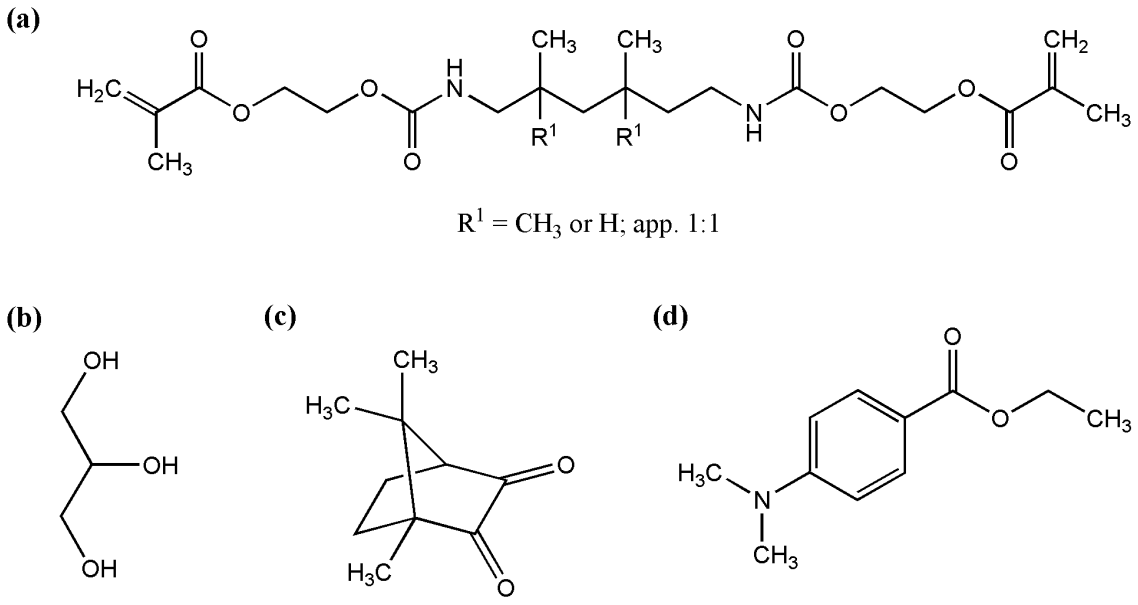

Fig. 1 Molecular structures of the substances used to prepare the monomeric mixtures: **(a)** UDMA; **(b)** glycerol; **(c)** CQ; **(d)** ethyl-*p*-dimethylaminobenzoate.

Photopolymerization

Each monomeric mixture was placed in a Teflon mold (1.5 mm in depth and 3.0 mm in diameter) and then photopolymerized by exposing to a light emitting diode (LED, D-2000, DMC Ltd., São Carlos, SP, Brazil). This LED emits blue light (1 W cm^{-2}) in the region of 430-490 nm. Samples were irradiated for a total of 400 s. The final polymers (1:5 of UDMA:glycerol) were named depending on the metal oxide filled in the structure: PUMG-Al_2O_3, PUMG-TiO_2, PUMG-Nb_2O_5, PUMG-La_2O_3 and PUMG-ZrO_2.

Sample characterization

Thermal analysis: simultaneous thermogravimetry differential thermal analysis (TG-DTA) and differential scanning calorimetry (DSC)

Simultaneous TG-DTA curves for each polymer were obtained using a Netzsch thermal analysis system (model STA 449 F3). Samples were analyzed in a 200-mL α-alumina open crucible with approximately 15 mg of sample. Samples were heated from 30.0 to 800.0 ºC, at a heating rate of 10.0 °C min^{-1}, and with a flow rate of 50.0 mL min^{-1} of a dry air atmosphere. The first derivative (DTG) peak is shown alongside the TG curves to improve the visualization of mass losses.

DSC analyses were performed using a Mettler-Toledo DSC (model DSC 1 Star^e System) using a 40-μL closed aluminum crucible with a perforated lid. Analysis was performed with 10 mg of sample without any previous thermal treatment. Samples were initially cooled from 25 ºC to -35 ºC, and maintained at -35 ºC for 10 min, before heating from -35 ºC to 145 ºC. This cycle of cooling and heating was performed two times, with a heating rate of 10.0 °C min^{-1} and a flow rate of 50.0 mL min^{-1} in a dry air atmosphere.

All samples were analyzed using the same heating and cooling steps, due to similarity in thermal stability between the samples.

Middle infrared spectroscopy (MIR)

Monomer conversion percentage (MC) was calculated using a Bruker spectrophotometer (model Vertex 700) operating in the range of 1680-1500 cm^{-1}. A drop of the monomeric mixture was placed over the diamond crystal and then irradiated with a light emitting diode (LED, D-2000, DMC Ltd., São Carlos, SP, Brazil) for 400 s. Transmittance (*T*%) spectra were collected every 10 s, resulting in 40 measurements for each polymer. Transmittance values were used to calculate MC values according to Equation (1) [15,16,24,25].

$$MC\ (\%) = \left[1 - \left(\frac{T_{t=x(C=C)}}{T_{t=0(C=C)}}\right)\right] \times (-1000) \quad (1)$$

MC was calculated using the transmittance of carbon-carbon double bonds (C=C). In the middle infrared spectra, the C=C bond wavenumber is found at approximately 1640 cm^{-1}. At the initial time (t=0), a minimum transmittance is observed at this wavenumber, since the carbon double bonds of the monomers have not yet been cleaved. Transmittance values of the C=C bond increase over time every 10 seconds (t=x, where x = seconds), as these bonds are cleaved by a radical initiator and polymerization occurs. By using this data and Eq. (1), it was possible to plot a graph of MC versus time. In addition, the rate of polymerization was calculated via a subtraction process, by calculating differences in MC values between 10 s intervals (for example at t=30 s, rate of polymerization is MC at t=30 s minus the MC value at t=20 s) using a previously reported method in the literature [25].

Scanning electronic microscopy (SEM)

Polymer morphology was studied using an EVO LS15 scanning electronic microscope from Zeiss. Samples were macerated into small pieces, placed over a SEM standard carbon adhesive and plated with gold. The voltage was set at 15 kV and samples were analyzed, in a high vacuum environment (10^{-3} Pa), at x 300 and x 700 magnification.

Results and discussion

Photopolymerization

In order to form free radical initiators, the photosensitizer CQ was radiated with (and thus absorbed) light at a wavelength of 400-550 nm, in order to reach an excited electronic state. This enables the molecule to abstract a hydrogen atom from the co-initiator ethyl-*p*-dimethylaminobenzoate, then it becomes a primary radical. Although CQ also turns into a radical species, the resonance in its structure due to the second carbonyl group stabilizes the molecule, thus narrowing its potential to cleave the carbon double bonds [16]. The proposed reaction mechanism of photochemical radical initiation is illustrated in Fig. 2a. Meanwhile, glycerol in the monomeric mixture can also become a radical initiator. Once in an

excited state, CQ can also withdraw a hydrogen atom from the secondary carbon atom of glycerol, creating another free radical initiator (Fig. 2b) [15,16,26]. As a result, two radical initiators are formed that can take part in the polymerization process (Fig. 2c). Both radicals can start the radical polymerization process, by promoting homolytic cleavage of the π carbon bonds (C=C) of the UDMA monomers [8-10,12]. The glycerol radical may also dehydrate to form radical alkene compounds as reported in the literature [27-29]. The importance of this process will be discussed in more detail later.

After the formation of the radical initiators, there are two options of bonding to the monomers. The most stable conformation occurs when the initiator attacks the primary carbon of the π carbon bond and a tertiary radical is formed. The formation of a primary radical is possible but is less stable (Fig. 3a) [12,15,16,26]. Thereafter, the radical monomer undergoes propagation, by reacting with more UDMA monomers and thus forming a radical oligomer (Fig. 3b). Finally, the termination phase occurs when any two radical species react together. After the photopolymerization process, all samples were rigid solids at room temperature. Fig. S1 in the Supplementary Material exhibits the monomeric mixtures and their respective final polymers after the photopolymerization process.

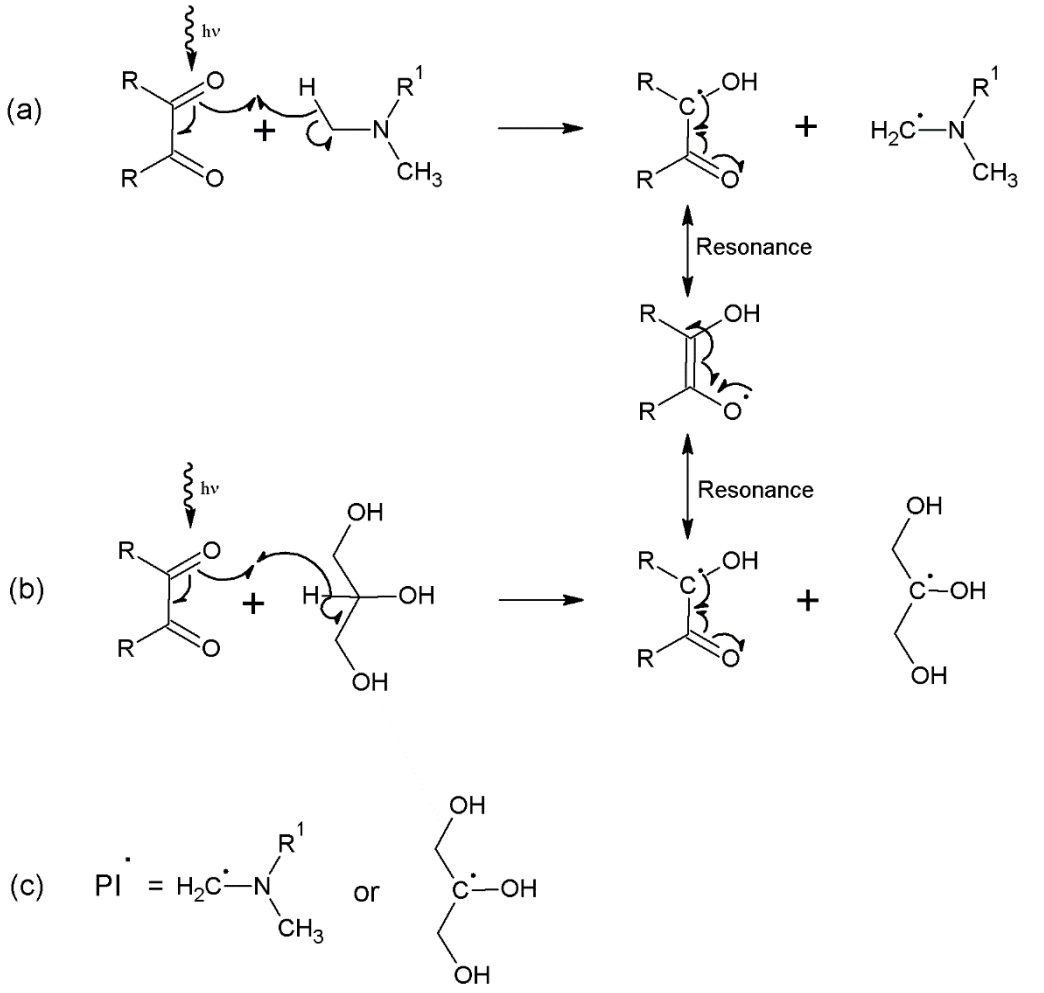

Fig. 2: Proposed reaction mechanism of photochemical radical initiator (PI˙) formation: **(a)** CQ reaction with the tertiary amine of ethyl-p-dimethylaminobenzoate; **(b)** CQ reaction with glycerol; **(c)** photoinitiating species used in this process.

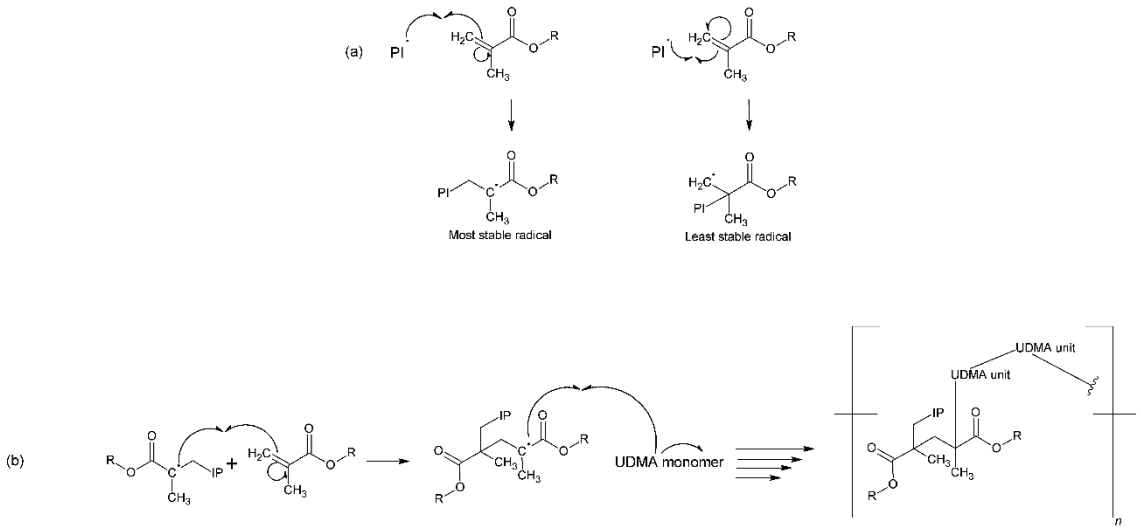

Fig. 3 Proposed mechanism for **(a)** the initiation step of monomer polymerization; **(b)** the propagation step and oligomer formation.

TG-DTA and DSC

As previously reported in the literature [15], the TG/DTG curves of the UDMA polymer with glycerol (1:5) presented five mass loss steps. The first one corresponds to the evaporation of acetone and water (formed as a by-product in the reaction), followed by four mass loss steps associated with polymer degradation, respectively. The UDMA polymer with glycerol (1:5) was thermally stable up to 147.2 ºC. Although, the TG curve exhibits only three steps related to polymer decomposition, it is possible to observe in the DTG curve that the first decomposition step (the second mass loss step in the TG curve) is a complex and overlapped decomposition.

In this study, TG/DTG curves of the synthesized polymers illustrated that all polymers were stable with slight variations in stability temperature between them (Table 1). All metal oxide filled polymers exhibited similar thermal behavior, with five consecutive mass loss steps related to the same events as reported for the UDMA:glycerol polymer (1:5). The first mass loss steps, as observed for the UDMA:glycerol polymer (1:5), relates to the evaporation of acetone and water. The others mass losses were associated with polymer degradation. This occurred with all metal oxide polymer samples. The PUMG-Al_2O_3 polymer (Fig. 4a) presented the highest thermal stability and was stable up to 158.5 ºC, whereas PUMG-TiO_2 (Fig. 4b), PUMG-Nb_2O_5 (Fig. 4c), PUMG-La_2O_3 (Fig. 4d) and PUMG-ZrO_2 (Fig. 4e) polymers were stable up to 134.0, 142.2, 144.9 and 138.8 °C, respectively.

The second, third, fourth and fifth mass loss steps were similar for all samples and are related to polymer degradation and associated with exothermic events in the DTA curves. Furthermore, all polymers presented a final total decomposition temperature close to the UDMA: glycerol (1:5) polymer without oxide filler (607.5 ºC) [15]. Each polymer left a residual mass in the crucible after TG analysis due to the presence of metal oxides (as shown in Table 1), confirming the amount of oxide added was approx. 5.0 (wt%) as described for each material. The slight differences between added oxide amount and oxide mass detected via TG analysis can be related to equipment error (± 0.5%).

The DSC curves for all polymers samples were very similar (Fig. 5a-e). In the cooling cycles, no events were observed for all samples. In the first heating cycle, every polymer presented an endothermic

event associated with an evaporation process, whilst exhibiting similar enthalpy values. In the second heating step, no thermal event was observed. The endothermic process in the first heating cycle was related to the mass loss reported at the same temperature range in the TG curves. The fact that this event did not occur again during the second heating cycle is indicative that this event is related to the evaporation of solvent and water. The enthalpy values (ΔH) related to these endothermic events for PUMG-Al_2O_3, PUMG-TiO_2, PUMG-Nb_2O_5, PUMG-La_2O_3 and PUMG-ZrO_2 were 106.6, 100.6, 102.7, 95.6 and 95.2 J g^{-1}, respectively. These enthalpy values were significantly higher than reported for the standard UDMA:glycerol (1:5) polymer, which presented an evaporation enthalpy value equal to 16.3 J g^{-1} [15]. Therefore, these enthalpy values correlate to more water production due to glycerol dehydration and consequently more radical formation, which assists with monomer conversion.

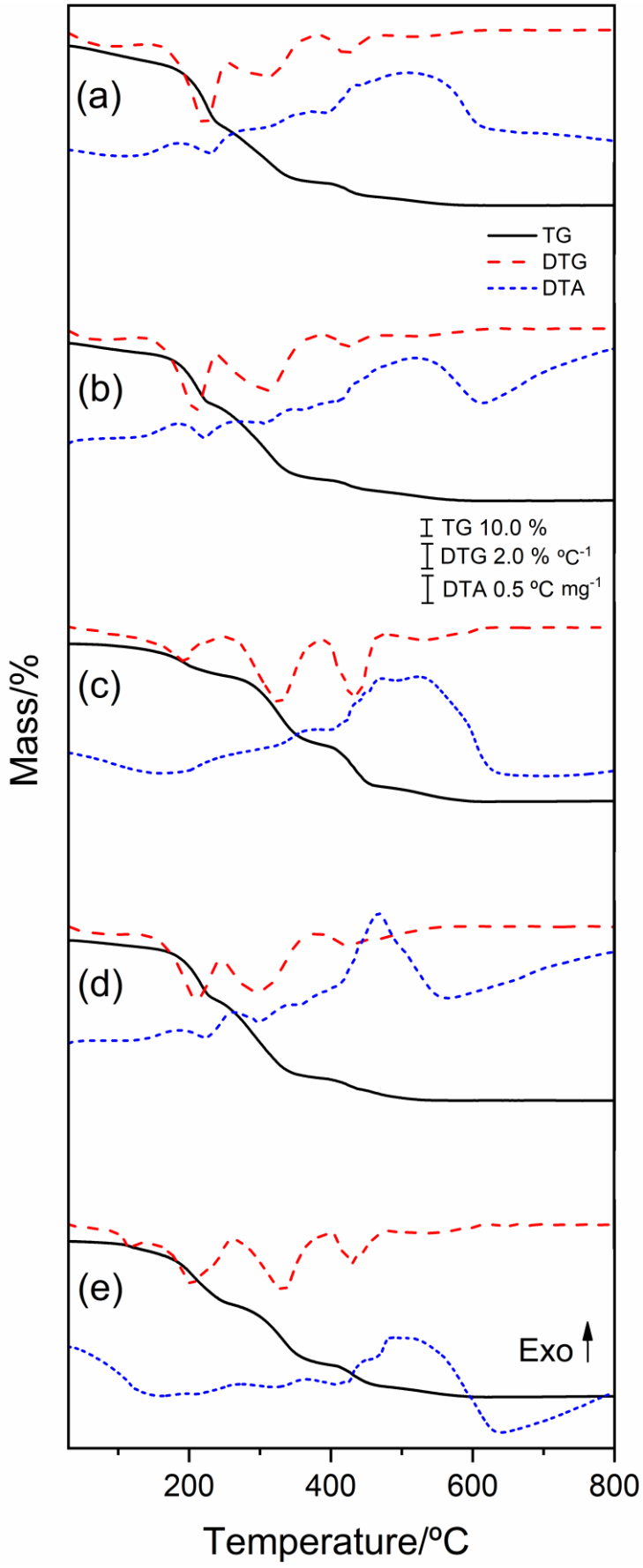

Fig. 4 TG/DTG-DTA curves for **(a)** PUMG-Al_2O_3; **(b)** PUMG-TiO_2; **(c)** PUMG-Nb_2O_5; **(d)** PUMG-La_2O_3; **(e)** PUMG-ZrO_2.

Table 1 Thermal events observed in each TG-DTA curve.

Polymers		1st step	2nd step	3rd step	4th step	5th step	Residual mass (%)
PUMG-Al_2O_3	θ/°C	30.0-158.5	158.5-249.4	249.4-392.2	392.3-464.3	464.3-596.8	4.61
	Δm/%	11.21	34.37	33.80	9.46	6.55	
	T_P/°C	-	184.3 ↑	252.8-279.0 *; 344.7-382.7 *	437.4 ↑	509.7 ↑	
PUMG-TiO_2	θ/°C	30.0-142.2	142.2-234.0	234.0-383.7	383.7-456.6	456.6-595.8	4.85
	Δm/%	6.27	30.64	45.18	6.73	6.33	
	T_P/°C	-	185.5 ↑	246.1-269.4 *; 332.9-351.9 *	-	521.6 ↑	
PUMG-Nb_2O_5	θ/°C	30.0-134.0	134.0-249.4	249.1-386.1	386.1-471.0	471.0-601.1	4.66
	Δm/%	3.08	16.09	41.74	25.46	8.97	
	T_P/°C	-	-	369.1 ↑	472.0 ↑	523.2 ↑	
PUMG-La_2O_3	θ/°C	30.0-144.9	144.9-241.6	241.6-380.8	380.8-442.3	442.3-547.5	4.91
	Δm/%	4.43	31.86	45.12	7.05	6.63	
	T_P/°C	-	186.3 ↑	264.2 ↑; 324.4-350.8 *	-	467.5 ↑	
PUMG-ZrO_2	θ/°C	43.9-138.8	138.8-258.7	258.7-398.2	398.2-475.1	475.1-607.5	4.94
	Δm/%	5.34	32.40	36.86	13.54	6.92	
	T_P/°C	-	191.9 ↑	273.1 ↑ 365.2 ↑	413.0-425.5* 425.5-460.4*	488.8 ↑	

θ = Temperature range; Δm = mass loss; T_P = temperature peak; ↑ = exothermic peak; * = exotherm.

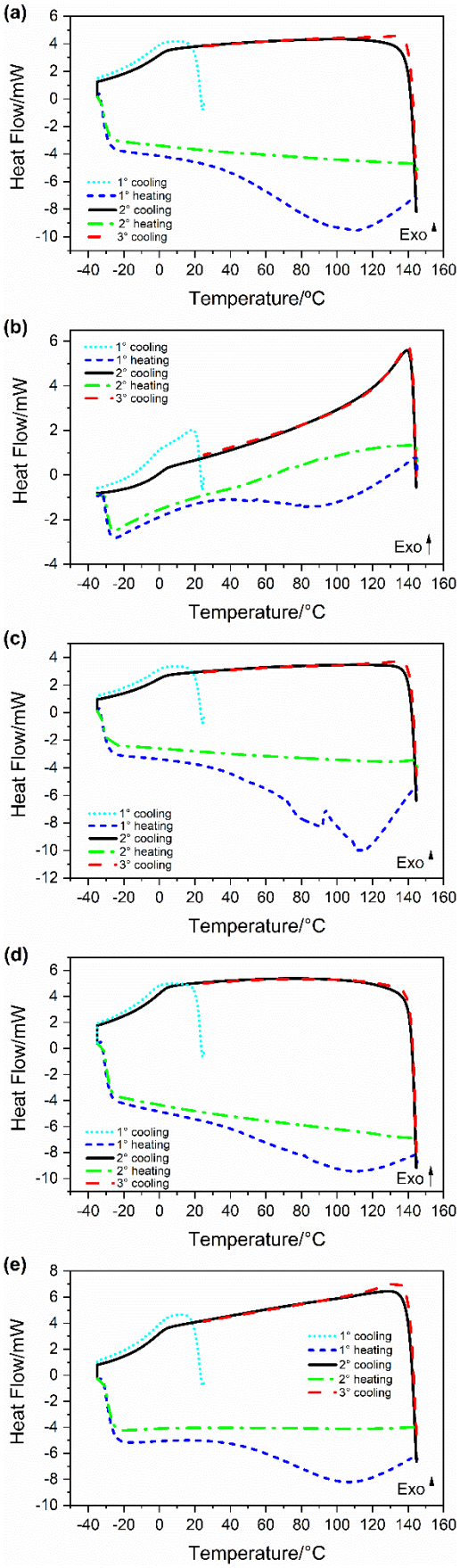

Fig. 5 DSC curves **(a)** PUMG-Al_2O_3; **(b)** PUMG-TiO_2; **(c)** PUMG-Nb_2O_5; **(d)** PUMG-La_2O_3; **(e)** PUMG-ZrO_2.

MIR

Monomer conversion values were calculated from MIR spectra using Eq. (1) and collecting a spectrum every 10 s up to 400 s. By plotting MC results against time (Fig. 6a) the respective rates of polymerization (Rp_{max}) could also be plotted (Fig. 6b). Example MC values obtained for the different polymers overtime are shown in Table 2. The PUMG-Al_2O_3 polymer had the highest MC value (87.42%) reported out of all polymer samples, followed by PUMG-TiO_2 (78.47%), PUMG-Nb_2O_5 (77.64%) and PUMG-La_2O_3 (75.51%). Polymers with aluminum, titanium and niobium oxides reported higher MC values than polymerizing UDMA without glycerol (75.83%), as previously reported in the literature under identical reaction conditions [15]. All four metal oxide filled polymers presented significantly higher MC values than the UDMA:glycerol (1:5) polymer (67.52%) [15]. The only exception was PUMG-ZrO_2, which reported a smaller MC value (52.52%).

Despite aluminum, titanium, niobium and lanthanum oxides reporting similar monomer conversions, the speed of polymerization was different for PUMG-TiO_2 (Fig. 6b), with a slow conversion of only 6.42% after 10 s. The lanthanum, aluminum, niobium and zirconium oxide filled polymers reported 40.54, 40.09, 33.35 and 31.99% conversion at the same time point, respectively. Only after 280 s did the PUMG-TiO_2 polymer start exhibiting higher conversions than reported for the PUMG-Nb_2O_5 polymer. The La_2O_3, Al_2O_3, Nb_2O_5 and ZrO_2 filled polymers reached their Rp_{max} values in the first 20 s, while the TiO_2 filled polymer reached its Rp_{max} point at 40 s (Fig. 6b). This could be due to its low dispersion in the monomer mixture, as shown in Fig. S1-b in the Supplementary Material.

As none of the metal oxides used absorb light with a wavelength of 430-490 nm, the generation of electron-hole pairs on the metal oxide surfaces, which would lead to radical formation and monomer cleavage, could not be responsible for the increase in MC values [31-35]. When the MC values are correlated with the first mass loss steps observed in the TG/DTG curves, the PUMG-Al_2O_3 polymer exhibited the highest mass loss and conversion values (Δm=11.60% and MC=87.42%, respectively), whilst all other samples exhibited mass loss values lower than 7.0%.

As previously mentioned, the glycerol radical can dehydrate to form an alkene and water [27,28]. With this in mind, it is possible that Al_2O_3 could have acted as a catalyst for the dehydration of the glycerol radical. This reaction has an activation energy of 65.2-70.9 kcal mol^{-1} for glycerol, which nearly halves for protonated glycerol (24.9-36.2 kcal mol^{-1}) [27]. It can therefore be predicted that a glycerol radical would have an even smaller activation energy, as it is less stable state of glycerol. Under the presence of a metal oxide, which has acidic sites and acidic properties [36-38], dehydration of the radical glycerol could have been catalyzed during the polymerization process. The consequent formation of alkenes means that these π carbon bonds may have been cleaved in the polymerization process and incorporated into the polymeric chain. Lastly, PUMG-ZrO_2 had the smallest MC value and was even lower than reported for the standard UDMA:glycerol (1:5) polymer made without the addition of any fillers [15]. This demonstrates that this oxide negatively disturbed the polymeric system, perhaps by inhibiting the interaction between the radical initiators and the monomers. This is probably related to the poor-dispersion of ZrO_2 in the monomeric mixture, as observed by its dispersion in the medium before the photopolymerization process (Fig. S1 in Supplementary Material).

It can be seen that the Al_2O_3 (Fig. S1-a) and Nb_2O_5 (Fig. S1-c) oxides were well dispersed in the reaction medium. It is important to emphasize that the Al_2O_3 system was so efficient in the polymerization of UDMA, that the polymerization process started after only a few seconds. Nevertheless, the sample with La_2O_3 (Fig. S1-d) exhibits some white agglomerates, like the ZrO_2 sample (Fig. S1-e), suggesting the particles are suspended in the monomeric mixture, exhibiting several non-homogeneous oxides clusters. It is therefore possible that higher MC values correlate with the dispersion of the oxides in the monomeric mixture, which in turn relates to the physical intermolecular interactions between the oxides and monomer solutions. Previous literature reports that the incorporation of methacrylate monomers onto oxide surfaces can lead to chemical modifications of the oxide. These modified oxides can then be applied in photopolymerization reactions to form a polymeric matrix that is chemically bonded to the metal oxide (or fillers) [39,40]. Another way to provide polymers with chemical bonding between the monomer and metal is by using metallic ion, which can act as crosslinkers between polymeric chains. In this study, none of the metal oxides or methacrylate monomers have undergone chemical modification prior to the polymerization reaction. Therefore, the monomers made in this work are predicted to interact with the polymeric crosslinked matrix via physical interactions [39,40].

In addition, this hypothesis is supported by analyzing the MIR spectra obtained for the monomeric mixture made with Al_2O_3 and PUMG-Al_2O_3, as shown in Fig. S2 and S3 (Supplementary Information). Principal bands that could change due to chemical bonding occurring between the monomer and metal oxide are highlighted in Fig. S2 and S3. These bands do not show any changes in intensity or any shifts in wavenumber after polymerization. The band at 3365 cm^{-1} is related to the O-H stretch in glycerol or water and did not change after polymerization (highlighted in red, Fig. S2). Furthermore, both the C=O band at 1706 cm^{-1} (highlighted in blue, Fig. S3) and the band for N-C=O at 1604 cm^{-1} (shown by a green arrow, Fig. S3) did not exhibit any changes (Fig. S3). Finally, only the C=C band of the methacrylate group at 1637 cm^{-1} changed after polymerization, which is to be expected (as shown by the red arrow)

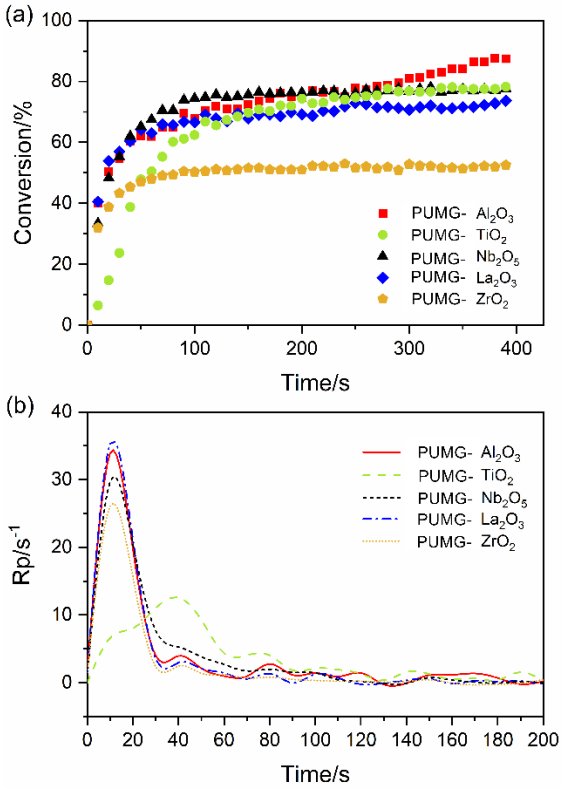

Fig. 6 (a) MC curves for synthesized polymers; **(b)** respective rates of polymerization.

Table 2 MC (%) values obtained for the five metal oxides filled polymers during the polymerization process

Polymers	10 s	50 s	100 s	250 s	400 s
PUMG-Al_2O_3	40.09	62.08	67.78	77.77	87.42
PUMG-TiO_2	6.42	47.82	62.38	74.69	78.47
PUMG-Nb_2O_5	33.35	65.15	74.41	76.16	77.64
PUMG-La_2O_3	40.54	64.14	66.57	72.89	75.51
PUMG-ZrO_2	31.99	47.00	50.29	51.60	52.52

SEM

As previously mentioned, it is suggested that Al_2O_3 increases the dehydration process of the glycerol radical, which releases more water into the reaction mixture compared to the other oxides. This is supported by the SEM images (Fig. 7), which shows sphere formation in all polymeric systems (especially at a magnification of x700). Sphere formation may be related to the UDMA polymer coating onto the oxide clusters due to the hydrophobicity of UDMA, which can create spheres when water is released in the glycerol dehydration process [2]. The PUMG-TiO_2 polymer (MC=78.47%) exhibited the largest spheres with small clusters on its surface, followed by PUMG-Nb_2O_5 (MC=77.64%, sphere diameter > 120 µm) and PUMG-La_2O_3 (MC=75.51%, sphere diameter between 19.7-100.5 µm). Lastly, the PUMG-ZrO_2 polymer (MC=52.52%) exhibited agglomerates on its surface, some of which were lamellar in shape and not well-defined. It is also possible to visualize some pores on its surface, which is characteristic of the UDMA:glycerol (1:5) polymer obtained in previous work, though this one did not show a spherical shape [15].

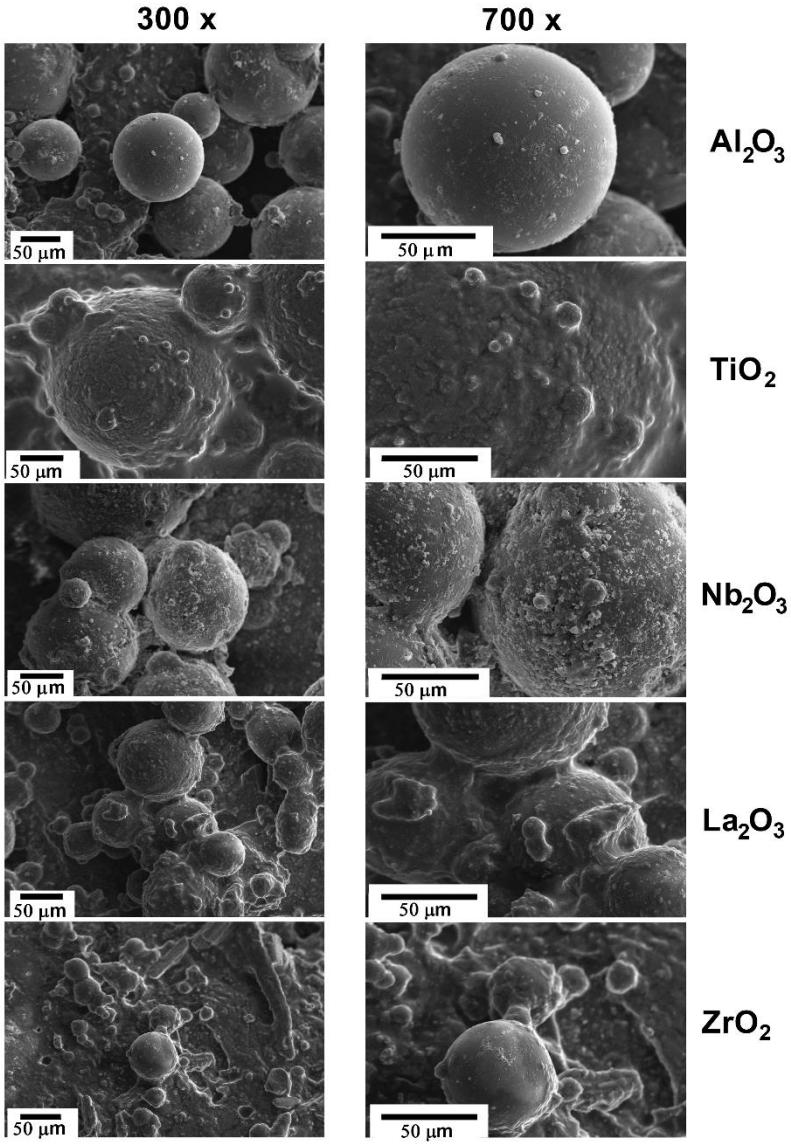

Fig. 7 SEM analysis of the Al_2O_3, TiO_2, Nb_2O_5, La_2O_3 and ZrO_2 filled polymers. Samples are shown at a magnification of ×300 (left) and ×700 (right).

Conclusions

The metal oxide-filled UDMA:glycerol (1:5) polymers were effectively synthesized via a photochemical route. This was performed using visible light to supply the energy required to generate free radical initiators. The addition of Al_2O_3, TiO_2, Nb_2O_5 and La_2O_3 was not detrimental to reporting high monomer conversions, obtaining conversions of 87.42, 78.47, 77.64 and 75.51%, respectively. It is important to emphasize that the Al_2O_3, TiO_2, Nb_2O_5 oxide filled polymers exhibited conversion values higher than reported when polymerizing UDMA without the addition of glycerol or metal oxide fillers (75.83%). The exception to this is the ZrO_2 metal oxide polymer, which reported 52.52% conversion, which was even lower than polymerizing UDMA with glycerol (67.52%). Except for the Al_2O_3 polymer, which presented a small increase in thermal stability of approximately 10 ºC, no significant changes were observed

in the thermal behavior of the final polymers. The variation of conversion values and Rp values were related to the homogenization of the oxides in the reaction medium. This was supported by SEM analysis of the monomeric mixtures after preparation, in which the spherical shapes were greater in these samples. This study also confirmed that the addition of metal oxide fillers, Al_2O_3, TiO_2 Nb_2O_5 and La_2O_3, in the UDMA:Glycerol polymeric structure can substantially enhance monomer conversion, without any significant changes in the thermal stability of the polymer. In summary, these results confirm that filling a polymeric structure with suitable metal oxides may lead to higher monomer conversions, thus providing an alternative way to improve UDMA polymeric materials with glycerol, which is an industrial waste that should be utilized more and used in the materials research field. Furthermore, this present work opens the possibility to create new polymers, which in turn should be studied in terms of their optical activity, electrical and thermal conductivity, photocatalytic effects and mechanical properties in future works.

References

[1] Marghalani HY (2015) Resin-based dental composite materials. In: Antoniac I. (eds) Handbook of Bioceramics and Biocomposites. Springer, Cham

[2] Barszczewska-Rybarek IM (2019) A guide through dental dimethacrylate polymer network structural characterization and interpretation of physico-mechanical properties. Mater 12: 40-57

[3] Melinte V, Buruiana T, Balan L, Buruiana EC (2012) Photocrosslinkable acid urethane dimethacrylates from renewable natural oil and their use in the design of silver/gold polymeric nanocomposites. React Funct Polym 72: 252-259

[4] Antonucci JM, Regnault WF, Skrtic D (2010) Polymerization shrinkage and stress development in amorphous calcium phosphate/urethane dimethacrylate polymeric composites. J Compos Mater 44: 355-367

[5] Nguyen JF, Pomes B, Sadoun M, Richaud E (2019) Curing of urethane dimethacrylate composites: a glass transition study. Polym Test 80: 106-113

[6] Guo X, Cheng Q, Wang H, Yu G, Tian Z, Shi Z, Cui Z, Zhu S (2020) Synthesis, characterization, and aging resistance of the polyurethane dimethacrylate layer for dental restorations. Eur J Oral Sci. https://doi.org/10.1111/eos.12674

[7] Xu Y, Wang H, Xie D (2018) Preparation of new low viscosity urethane dimethacrylates for dental composites. J Biomater Sci, Polym Ed 29: 1011-1025

[8] Lalevée J, Fouassier JP (2015) Dyes and chromophores in polymer science. ISTE, London

[9] Fouassier JP, Lalevée J (2012) Photoinitiators for polymer synthesis: scope, reactivity and efficiency. Wiley, Germany

[10] Allonas X, Lalevée J, Fouassier, JP (2003) Investigation of cleavage processes in photoinitiators: from experiments to molecular modeling. J Photoch Photobio A 159: 127–133

[11] Tehfe MA, Louradour F, Lalevée J, Fouassier JP (2013) Photopolymerization reactions: on the way to a green and sustainable chemistry. Appl Sci 3: 490-514

[12] Fouassier JP, Allonas X, Burget D (2003) Photopolymerization reactions under visible lights: principle, mechanism and examples of applications. Prog Org Coat 47: 16-36

[13] Anastas P, Eghbali N (2010) Green chemistry: principles and practice. Chem Soc Rev 39: 301-312
[14] Sheldon RA (2008) E factors, green chemistry and catalysis: an odyssey. Chem Commun 29: 3352-3365
[15] Alarcon RT, Gaglieri C, Bannach G (2018) Dimethacrylate polymers with different glycerol content. J Therm Anal Calorim 132: 1579-1591
[16] Alarcon RT, Holanda BBC, Rinaldo D, Caires FJ, Almeida MV, Bannach G (2017) Synthesis thermal studies and conversion degree of dimethacrylate polymers using new non-toxic coinitiators. Quim Nova 40: 363-370
[17] Gu Y, Jérôme F (2010) Glycerol as a sustainable solvent for green chemistry. Green Chem 12: 1127-1138
[18] Análise de conjuntura dos biocombustíveis ano 2018 (2019) Ministério de Minas e Energia, Rio de Janeiro. http://www.epe.gov.br. Acessed 01 Jun 2020
[19] Habib E, Wang R, Wang Y, Zhu M, Zhu XX (2016) Inorganic fillers for dental resin composites: present and future. ACS Biomater Sci Eng 2: 1-11
[20] Móczó J, Pukánszky B (2008) Polymer micro and nanocomposites: structure, interactions, properties. J Ind Eng Chem 14: 535-563
[21] Turssi CP, Ferracane JL, Vogel K (2005) Filler features and their effects on wear and degree of conversion of particulate dental resin composites. Biomater 26: 4932-4937
[22] Melinte V, Buruiana T, Chibac A, Lupu N, Grigoras M, Buruiana EC (2015) Preparation and properties of photopolymerized hybrid composites with covalently attached magnetite nanoparticles. Chem Eng J 259: 542-551
[23] Chibac AL, Melinte V, Buruiana T, Mangalagiu I, Buruiana EC (2015) Preparation of photocrosslinked sol-gel composites based on urethane-acrylic matrix, silsesquioxane sequences, TiO_2, and Ag/Au nanoparticles for use in photocatalytic applications. Polym Chem 53: 1189-1204
[24] Alarcon RT, Gaglieri C, de Oliveira AR, Bannach G (2018) Use of DSC in degree of conversion of dimethacrylate polymers: easier and faster than MIR technique. J Therm Anal and Calorim 132: 1423-1427
[25] Alarcon RT, Dos Santos GC, de Oliveira AR, Silva-Filho LC, Bannach Gilbert (2019) Synthesis of luminescent polymers in the UV light region from dimethacrylate monomer using novel quinoline dyes. J Appl Polym Sci 136: 47461-47468
[26] De Oliveira DSBL, De Oliveira LSBL, Alarcon RT, Holanda BBC, Bannach G (2017) Use of curcumin and glycerol as an effective photoinitiating system in the polymerization of urethane dimethacrylate. J Therm Anal Calorim 128: 1671-1682
[27] Nimlos MR, Blanksby SJ, Qian X, Himmel ME, Johnson DK (2006) Mechanism of glycerol dehydration. J Phys Chem A 110: 6145-6156
[28] Katryniok B, Paul S, Bellière-Baca V, Rey P, Dumeignil F (2010) Glycerol dehydration to acrolein in the context of new uses of glycerol. Green Chem 12: 2079-2098
[29] Yun D, Yun YS, Kim TY, Park H, Lee JM, Han JW, Yi J (2016) Mechanistic study of glycerol dehydration on Brønsted acidic amorphous aluminosilicate. J Catal 341: 33-43
[30] Bannach G, Cavalheiro CCS, Calixto L, Cavalheiro ETG (2015) Thermoanalytical study of monomers: BisGMA, BisEMA, TEGDMA UDMA and their mixture. Braz J Therm Anal 4: 28-34

[31] Filatova EO, Konashuk AS (2015) Interpretation of the changing the band gap of Al_2O_3 depending on its crystalline form: connection with different local symmetries. J Phys Chem C 119: 20755-20761
[32] Kambur A, Pozan GS, Boz I (2012) Preparation, characterization and photocatalytic activity of TiO_2-ZrO_2 binary oxide nanoparticles. Appl Catal B 115-116: 149-158
[33] Cheng JB, Li AD, Shao QY, Ling HQ, Wu D, Wang Y, Bao YJ, Wang M, Liu ZG, Ming NB (2004) Growth and characteristics of La_2O_3 gate dielectric prepared by low pressure metalorganic chemical vapor deposition. Appl Surf Sci 233: 91-98
[34] Lopes OF, Paris EC, Ribeiro C (2014) Synthesis of Nb_2O_5 nanoparticles through the oxidant peroxide method applied to organic pollutant photodegradation: a mechanistic study. Appl Catal B 144: 800-808
[35] Salinas D, Sepúlveda C, Escalona N, GFierro JL, Pecchi G (2018) Sol-gel La_2O_3-ZrO_2 mixed oxide catalysts for biodiesel production. J Energy Chem 27: 565-572
[36] Wang Z, Wang L, Jiang Y, Hunger M, Huang J (2014) Cooperativity of Brønsted and Lewis acid sites on zeolite for glycerol dehydration. ACS Catal 4: 1144-1147
[37] Masih D, Rohani S, Kondo JN, Tatsumi T (2019) Catalytic dehydration of ethanol-to-ethylene over Rho zeolite under mild reaction conditions. Micropor Mesopor Mater 282: 91-99
[38] Song Y, Xu S, Ling F, Tian P, Ye T, Yu D, Chu X, Lin Y, Yang X, Tang J (2017) Atomic layer deposition of aluminium on anatase: a solid acid catalyst with remarkable performances for alcohol dehydration. Catal Commun 99: 34-38
[39] Habib E, Wang R, Wang Z, Zhu M, Zhu XX (2016) Inorganic Fillers for dental resin composites: Present and Future. ACS Biomater Sci Eng 2:1-11
[40] Utech S, Boccaccini AR (2016) A review of hydrogel-based composites for biomedical application: enhancement of hydrogel properties by addition of rigid inorganic fillers. J Mater Sci 51:271-310